

Ultra-Wideband Balanced Bandpass Filters Based on Transversal Signal-Interference Concepts

Chaoying Zhao¹, Wenjie Feng^{1*}, Yuanchuan Li^{2,3}, and Wenquan Che¹

¹Department of Communication Engineering, Nanjing University of Science & Technology, Nanjing, China

²School of Electronic and Information Engineering, South China University of Technology, Guangzhou, China

³State Key Laboratory of Millimeter Waves, Southeast University, Nanjing, China

fengwenjie1985@163.com

Abstract — Two ultra-wideband balanced bandpass filters based on transversal signal-interference concepts are proposed in this paper. By employing the two structures: microstrip/slotline transition, and quarter-wavelength shorted coupler lines, 180° phase shift can be easily implemented for each design. In addition, due to the different transmission paths, wideband common mode rejection and differential mode transmission bandwidth can be achieved. Two balanced filters centered at 3 GHz are calculated, fabricated and measured successfully. For the differential mode, the 3-dB fractional bandwidths are 102% from 1.47 GHz to 4.53 GHz and 103% from 1.52 GHz to 4.61 GHz, respectively, and the return loss are both greater than 20 dB. For the common mode, signals are suppressed below -20 dB and -15 dB over the whole frequency band.

Index Terms — Balanced filter, differential/common mode, shorted stubs, Ultra-wideband.

I. INTRODUCTION

RF circuits and systems are becoming a complicated closer space with more functions. So, the electromagnetic interference between nodes at different dielectric layers and mutual link in communication systems to be eliminated is indispensable. Compared to single-ended technology, balanced circuits have advantages of wideband common mode rejection capability which is beneficial to immunity to the environmental noise and dynamic range.

As a high performance balanced circuit, only the differential mode signals pass through in the desired frequency band, while the common mode signals must be all-stop. In the past few years, different balanced filters for single-band, dual-band and wideband were proposed using different ways [1-8]. Chen et al. designed differential filter firstly with wideband common-mode suppression exploiting microstrip and CPW transition [1]-[3]. However, the differential-mode width increase difficulty and the insertion loss is a little big. Cascaded

branch-line was used to design wideband balanced filters as well [4]-[5]. However, these filters implied larger circuit size, and their out-of-band common mode suppression is not so good. Another way to get wideband balanced filter is using T-shaped structures [6]. Their main advantage is the high selectivity of the passband, but the suppression of common mode is always unsatisfactory. As a very convenient balanced transmission line for balanced circuits, DSPSL can be used to design ideal phase shifter for balanced filters [7]-[8]. They show good performance for the differential mode and common mode, but the problem of heat dissipation remained unsolved. In [9], a low profile balanced tunable BPF using $\lambda/2$ resonator has been presented. The common mode suppression can be kept at a high level by adding a varactor. In [10], it is a balanced SIW BPF which is simplified though designing a 2-port filter with high performance. But [9] and [10] both have the defect of differential-mode bandwidth.

II. ANALYSIS OF PROPOSED BALANCED FILTERS

In this part, the proposed two balanced filters based on transversal signal-interference concepts are illustrated detailedly. Firstly, we use the differential mode and common mode equivalent circuits to analyze their performance. And then, in *Part C*, simulated results of the two balanced filters are presented.

A. Balanced filter analysis with microstrip/slotline transition

The ideal circuit of the balanced filter with two ideal 180° phase shifter is shown in Fig. 1 (a). The transformer works as a phase shifter. We see that it is a central symmetric structure of all components. Specifically, there are two shunted $\lambda/4$ shorted lines loaded at four arms each, and the characteristic impedances of the input ports and output ports microstrip lines are all $Z_0 = 50 \Omega$. For the purpose of elaborate description, the equivalent circuits of the differential mode and common mode are

illustrated in Figs. 1 (b) and (c).

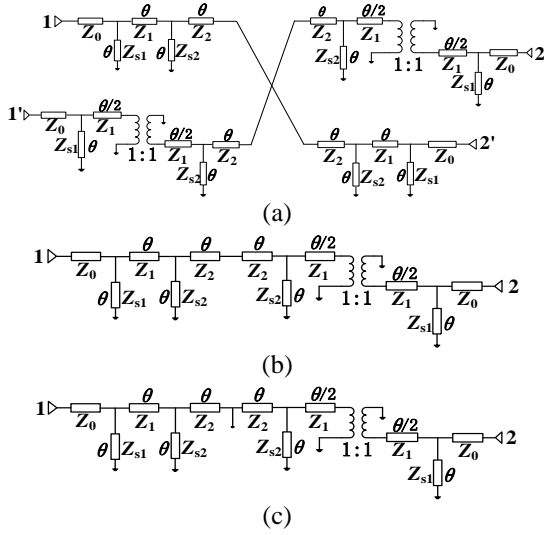


Fig. 1. (a) The ideal circuit of the balanced filter with microstrip/slotline transition, (b) equivalent circuit for the differential mode, and (c) equivalent circuit for the common mode.

When ports 1 and 1' are excited by differential mode signals, out-phase signals will be changed into in-phase signals after one kind phase of the signals pass through the phase converter. We can obtain $\theta_{12}(f_0) = 360^\circ$, $\theta_{1'2}(f_0) = 360^\circ$ ($\theta = 90^\circ$ at the center frequency f_0), then they are combined at the center point and propagate to output ports. The differential-mode circuit illustrated in Fig. 1 (b) shows that it is half of the circuit in Fig. 1 (a) due to the symmetrical structure. Besides, a virtual open appears at the joint of four arms. This means that the differential-mode circuit comes out a typical bandpass filter. The $ABCD$ matrix of the transmission lines and the shorted lines are:

$$M_{s1} = \begin{bmatrix} 1 & 0 \\ 1/jZ_{s1} \tan \theta & 1 \end{bmatrix}, \quad (1)$$

$$M_{s2} = \begin{bmatrix} 1 & 0 \\ 1/jZ_{s2} \tan \theta & 1 \end{bmatrix}, \quad (2)$$

$$M_1 = \begin{bmatrix} \cos \theta & jZ_1 \sin \theta \\ j \sin \theta / Z_1 & \cos \theta \end{bmatrix}, \quad (3)$$

$$M_2 = \begin{bmatrix} \cos 2\theta & jZ_2 \sin 2\theta \\ j \sin 2\theta / Z_2 & \cos 2\theta \end{bmatrix}, \quad (4)$$

$$M_{1/2} = \begin{bmatrix} \cos(\theta/2) & jZ_1 \sin(\theta/2) \\ j \sin(\theta/2) / Z_1 & \cos(\theta/2) \end{bmatrix}, \quad (5)$$

$$M_t = \begin{bmatrix} -1 & 0 \\ 0 & -1 \end{bmatrix}. \quad (6)$$

From port 1 to port 2, the $ABCD$ parameter matrix can be defined as $M_{s1} \times M_1 \times M_{s2} \times M_2 \times M_{s2} \times M_{1/2} \times M_t \times M_{1/2} \times M_{s1}$ derived from Equations (1) to (6). Then we can get the frequency response form $ABCD$ - to Y -parameter conversions. The poles, the insertion loss and bandwidth can be controlled by changing the transmission line impedances.

The simulated frequency responses of Fig. 1 (b) are shown in Fig. 2 (Simulated with ANSYS Designer v3.0). We can find that the transmission zero at both sides of the passband will not change with the characteristic impedance Z_{s1} and Z_{s2} . But Z_{s1} increased can improve performance of $|S_{dd11}|$ obviously in the passband. Without the two shorted lines of Z_{s1} , transmission poles decrease to three. As to Z_{s2} , it influences the bandwidth deeply, bigger Z_{s2} and bandwidth wider. But when it comes to the return loss in-band, the performance shows better first and then becomes worse with Z_{s2} increased. Although the bandwidth is much bigger, $|S_{dd11}|$ will down to 10 dB.

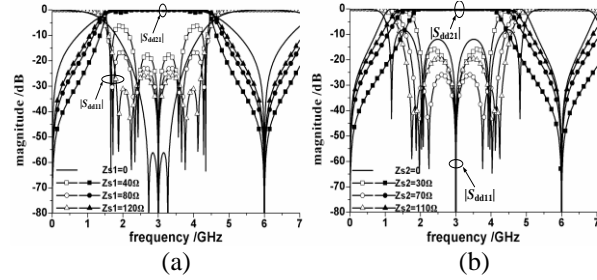


Fig. 2. Simulated frequency responses of Fig. 1 (b): (a) $|S_{cc11}|$ & $|S_{cc21}|$, $Z_1 = 50 \Omega$, $Z_2 = 70 \Omega$, $Z_{s2} = 70 \Omega$, and (b) $|S_{cc11}|$ & $|S_{cc21}|$, $Z_1 = 50 \Omega$, $Z_2 = 70 \Omega$, $Z_{s1} = 120 \Omega$.

When ports 1 and 1' are excited by common mode signals, similarly, in-phase signals will be changed into out-phase signals after one kind phase of the signals pass through the phase converter. That means input signals will be cancelled out at the center point, due to $\theta_{12}(f_0) = 180^\circ$ and $\theta_{1'2}(f_0) = 360^\circ$ ($\theta = 90^\circ$ at the center frequency f_0). In this case, the common mode circuit in Fig. 1 (c) is generated and there is a virtual short appears at the joint of four arms. Because common mode signals canceled at the joint, the circuit presents a stopband filter over the whole frequency band. So common mode signals suppression in/out-of-band for the differential mode is easy to achieve.

Figures 3 (a)-(b) plot the simulated frequency responses of Fig. 1 (c). As the two plots show that $|S_{cc11}|$ is almost steady over whole frequency band despite the characteristic impedance Z_{s1} and Z_{s2} change. But $|S_{cc21}|$ increased follows Z_{s1} or Z_{s2} increased. The performance becomes worse. Moreover, without the two shorted lines of Z_{s1} or Z_{s2} , $|S_{cc11}|$ and $|S_{cc21}|$ becomes worse than they existed.

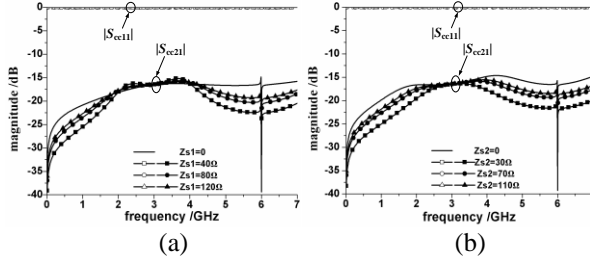


Fig. 3. Simulated frequency responses of Fig. 1 (c): (a) $|S_{cc11}|$ & $|S_{cc21}|$, $Z_1 = 50 \Omega$, $Z_2 = 70 \Omega$, $Z_{s2} = 70 \Omega$, and (b) $|S_{cc11}|$ & $|S_{cc21}|$, $Z_1 = 50 \Omega$, $Z_2 = 70 \Omega$, $Z_{s1} = 120$.

B. Balanced filter analysis with $\lambda/4$ shorted coupled line

Figure 4 (a) shows ideal circuit of the balanced filter, which is a central symmetric structure of all components. Figures 4 (b) and (c) are the equivalent differential/common mode circuits to be analyzed accordingly. We use $\lambda/4$ shorted coupled line in this circuit and its equivalent circuit model gives in Fig. 5. The $ABCD$ matrix can be written as follow:

$$\begin{bmatrix} A & B \\ C & D \end{bmatrix} = \begin{bmatrix} 1 & 0 \\ Y_{11} + Y_{12} & 1 \end{bmatrix} \begin{bmatrix} 1 & -Y_{12} \\ 0 & 1 \end{bmatrix} \begin{bmatrix} 1 & 0 \\ Y_{22} + Y_{12} & 1 \end{bmatrix} = \begin{bmatrix} -1 & 0 \\ 0 & -1 \end{bmatrix} \begin{bmatrix} Y_{11}/Y_{12} & 1/Y_{12} \\ (Y_{11}^2 - Y_{12}^2)/Y_{12} & Y_{11}/Y_{12} \end{bmatrix}, \quad (7)$$

$$\begin{bmatrix} -1 & 0 \\ 0 & -1 \end{bmatrix} = \begin{bmatrix} \cos(180^\circ) & jZ \sin(180^\circ) \\ jY \sin(180^\circ) & \cos(180^\circ) \end{bmatrix}, \quad (8)$$

$$Y_{11} = Y_{22} = -j(Y_{oo} + Y_{oe})/(2 \cdot \tan \theta_1), \quad (9)$$

$$Y_{12} = -j(Y_{oo} - Y_{oe})/(2 \cdot \sin \theta_1). \quad (10)$$

From the upper Equations from (7) to (10), we can draw a conclusion that the two $\lambda/4$ shorted coupled lines are acted as 180° phase shifter and will not change with frequency. The characteristic impedances of the input ports and output ports microstrip lines are all $Z_0 = 50 \Omega$.

As discussed in *Part A*, a virtual open appears at the joint of four arms for differential-mode circuit in Fig. 4 (b). Due to the signals combined at the center point, it comes out a typical bandpass filter when ports 1 and 1' are excited by differential mode signals. Furthermore, a virtual short appears at the joint of four arms for common-mode circuit in Fig. 4 (c). Due to the signals canceled at the center point, it comes out a stopband filter when ports 1 and 1' are excited by common mode signals.

Figures 6 (a) and (b) are the simulation results at different value of k . k is coupling coefficient of the two shorted coupler line. It is apparent that the differential mode and common mode performance show better with k increases. But there is a problem that big coupling coefficient is hard to realize in monolayer PCB microstrip line structure. In order to get tight coupling,

we introduce a slot under the coupled lines [12]. For a simple coupled line, even-mode impedance is mainly depend on capacitance of metal strips to ground, while odd-mode impedance is depend on capacitance of metal strips and coupled lines to ground. So even-mode and odd-mode capacitance will decrease with the slot at the same time. In addition, placing a rectangular conductor inside the slot can make sure that odd-mode decrease in company with even-mode.

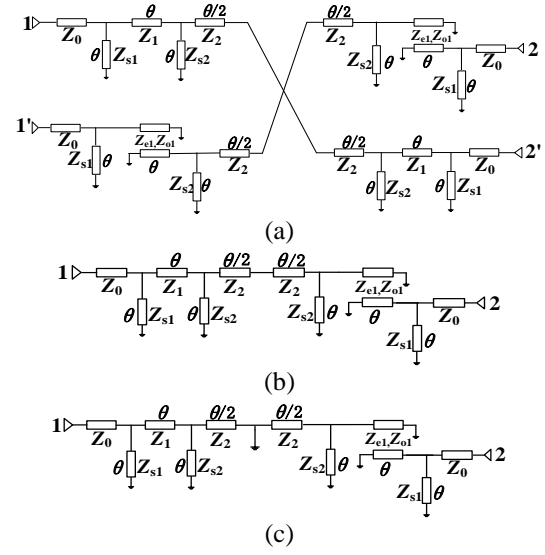


Fig. 4. (a) The ideal circuit of the balanced filter with $\lambda/4$ shorted coupled line, (b) equivalent circuit for the differential mode, and (c) equivalent circuit for the common mode.

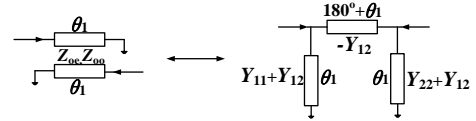


Fig. 5. Equivalent circuit model of the $\lambda/4$ shorted coupled line.

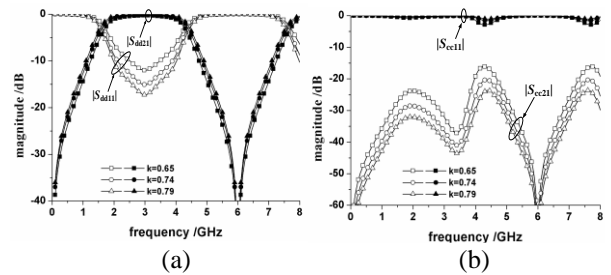


Fig. 6. Simulated frequency responses of Figs. 4 (b) and (c): (a) $|S_{dd21}|$ & $|S_{dd11}|$, $Z_1 = 55 \Omega$, $Z_2 = 65 \Omega$, $Z_{s1} = 120 \Omega$, $Z_{s2} = 120 \Omega$, and (b) $|S_{cc21}|$ & $|S_{cc11}|$, $Z_1 = 55 \Omega$, $Z_2 = 65 \Omega$, $Z_{s1} = 120 \Omega$, $Z_{s2} = 120 \Omega$.

C. Proposed to balanced bandpass filters

Based on the above discussions and the simulated results in Part A and B of Section II, the 3-dB bandwidths of the two balanced filters are chosen as 102% and 103%, and the final parameters in Figs. 1, 4 are: $Z_0=50\Omega$, $Z_1=50\Omega$, $Z_2=90\Omega$, $Z_{s1}=114\Omega$, $Z_{s2}=104\Omega$; $Z_0=50\Omega$, $Z_1=45\Omega$, $Z_2=60\Omega$, $Z_{s1}=112\Omega$, $Z_{s2}=112\Omega$, $Z_{c1}=200\Omega$, $Z_{o1}=30\Omega$. Figure 7 presents the geometries of the two balanced filters (78.94 mm \times 56.83 mm, 66.2 mm \times 37.28 mm) are: $l_1=16.85$ mm, $l_2=17.08$ mm, $l_3=9.93$ mm, $s_1=17.65$ mm, $s_2=18.42$ mm, $g_1=0.3$ mm, $l_g=7$ mm, $a=9.5$ mm, $b=2$ mm, $w_0=1.36$ mm, $w_1=1.36$ mm, $w_2=0.23$ mm, $w_3=0.3$ mm, $w_4=0.44$ mm, $d_1=0.6$ mm, $d_2=1$ mm, $d_3=10$ mm; $l_1=16.7$ mm, $l_2=17.7$ mm, $l_3=8.05$ mm, $s=0.15$ mm, $s_1=16.7$ mm, $s_2=16.7$ mm, $q_1=7.95$ mm, $q_2=14.7$ mm, $w_0=1.36$ mm, $w_1=2.1$ mm, $w_2=0.24$ mm, $w_3=1$ mm, $w_4=0.26$ mm, $g_1=1.6$ mm, $g_2=0.3$ mm, $d_1=0.6$ mm, $d_2=0.8$ mm.

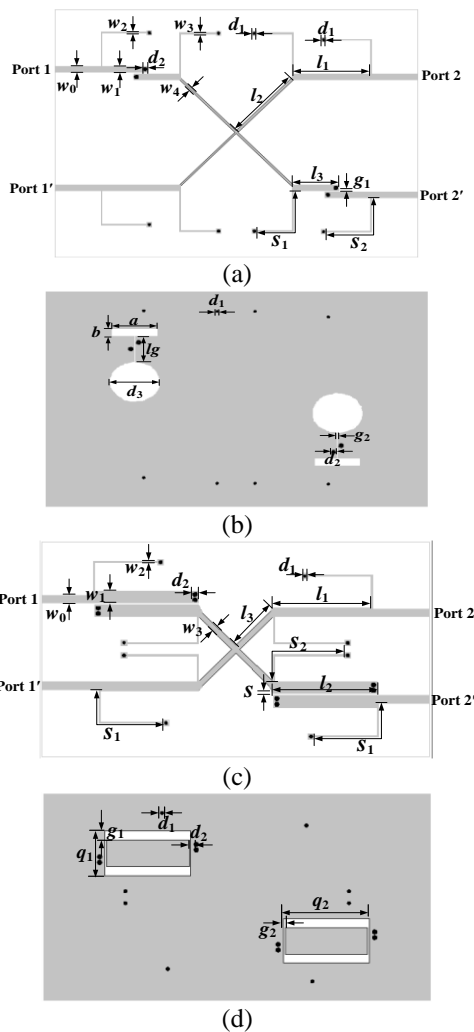


Fig. 7. Geometries of two proposed balanced filters. (a) Top view of structure I, (b) bottom view of structure I, (c) top view of structure II, and (d) bottom view of structure II.

The simulated results and photographs of the two balanced filters with two different 180° phase shifter are shown in Figs. 8 and 9 (Simulated with ANSYS HFSS v.11.0). As to the balanced filter with microstrip/slotline transition, the in-band insertion loss of differential mode is less than 1 dB with 3-dB bandwidth approximately 102% from 1.47 GHz to 4.53 GHz. And insertion loss of common mode is greater than 23 dB (0-5.7 GHz, $1.9f_0$), which manifested good wideband suppression. Furthermore, for the balanced filter with $\lambda/4$ shorted coupled line, 3-dB bandwidth is about 103% from 1.52 GHz to 4.61 GHz, meanwhile, the in-band insertion loss of differential mode is less than 1.3 dB. And insertion loss of common mode is greater than 15 dB (0-7.5 GHz, $2.5f_0$).

III. RESULTS AND DISCUSSION

Figures 8 and 9 present the measured results and photographs of the two balanced filters. We can see from Fig. 8 (a), 3-dB bandwidth is approximately 100% (1.47-4.48 GHz), the passband return loss is greater than 12.5 dB and insertion loss is less than 1.1 dB of the differential mode; for the common mode in Fig. 8 (b), a broadband rejection (0-7.5 GHz, $2.5f_0$) is achieved which up to 20 dB. The results of the second balanced filter are shown in Fig. 9, 3-dB bandwidth is approximately 100% (1.48-4.48 GHz), the passband return loss is greater than 11 dB and insertion loss is less than 1.3 dB of the differential mode; for the common mode in Fig. 9 (b), a broadband rejection (0-7.4 GHz, $2.46f_0$) is achieved which up to 15 dB. Aforementioned two structures, the in-band performance of differential mode has a bit discrepancy is mainly caused by the fabrication inaccuracy and errors of measurement.

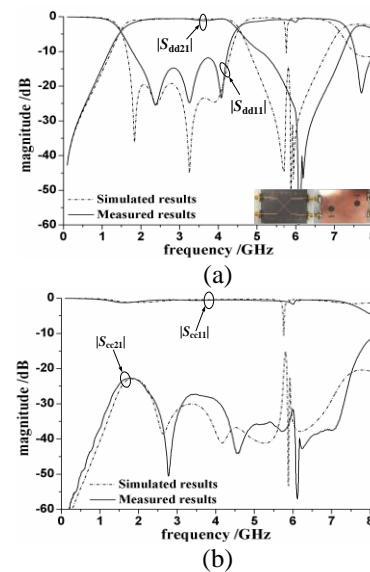


Fig. 8. Measured and simulated results of the balanced filter with microstrip/slotline transition. (a) Differential mode and (b) common mode.

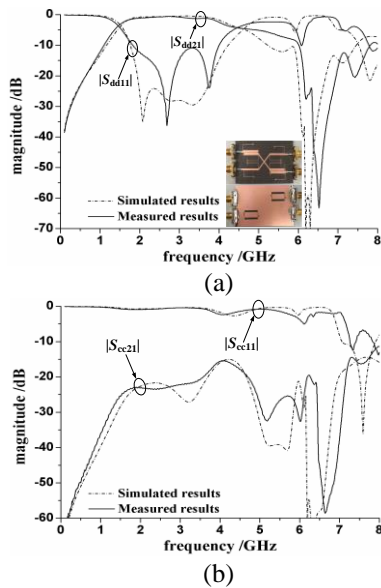


Fig. 9. Measured and simulated results of the balanced filter with $\lambda/4$ shorted coupled line. (a) Differential mode and (b) common mode.

IV. CONCLUSION

Two ultra-wideband balanced filters based on transversal signal-interference concepts are proposed in this paper. Wideband common mode signals suppression can be implemented conveniently for the filters with two structures, microstrip/slotline transition and quarter-wavelength shorted coupler lines. Then 180° phase shift realized therefore. It shows good performance for common mode suppression and little insertion loss of differential mode.

ACKNOWLEDGEMENT

This work is supported by the 2012 Distinguished Young Scientist awarded by the National Natural Science Foundation Committee of China (61225001), and by National Natural Science Foundation of China (6140010914, 61571231), Natural Science Foundation of Jiangsu Province (BK20140791) and the 2014 Zijin Intelligent Program of Nanjing University of Science and Technology.

REFERENCES

- [1] Y.-S. Lin and C. H. Chen, "Novel balanced microstrip coupled-line bandpass filters," in *Proc. URSI Int. Electromagn. Theory Symp.*, pp. 567-569, 2004.
- [2] C. H. Wu, C. H. Wang, and C. H. Chen, "Novel balanced coupled-line bandpass filters with common-mode noise suppression," *IEEE Trans. Microw. Theory Techn.*, vol. 55, no. 2, pp. 287-295, Feb. 2007.
- [3] C. H. Wu, C. H. Wang, and C. H. Chen, "Stopband-

extended balanced bandpass filter using coupled stepped-impedance resonators," *IEEE Microw. Wireless Compon. Lett.*, vol. 17, no. 7, pp. 507-509, July 2007.

- [4] T. B. Lim and L. Zhu, "A differential-mode wideband bandpass filter on microstrip line for UWB application," *IEEE Microwave Wireless Compon. Lett.*, vol. 19, no. 10, pp. 632-634, Oct. 2009.
- [5] T. B. Lim and L. Zhu, "Differential-mode ultra-wideband bandpass filter on microstrip line," *IET Electron. Lett.*, vol. 45, no. 22, pp. 1124-1125, Oct. 2009.
- [6] J. Shi and Q. Xue, "Balanced bandpass filters using center-loaded half-wavelength resonators," *IEEE Trans. Microw. Theory Techn.*, vol. 58, no. 4, pp. 970-977, Apr. 2010.
- [7] X. H. Wang, Q. Xue, and W. W. Chio, "A novel ultra-wideband differential filter based on double-sided parallel-strip line," *IEEE Microw. Wirel. Compon. Lett.*, vol. 20, no. 8, pp. 471-473, 2010.
- [8] J. Shi, J.-X. Chen, and Q. Xue, "A novel differential bandpass filter based on double-sided parallel-strip line dual-mode resonator," *Microw. Opt. Tech. Lett.*, vol. 50, no. 7, pp. 1733-1735, July 2008.
- [9] Q.-Y. Lu, J.-X. Chen, L.-H. Zhou, and H. Tang, "Novel varactor-tuned balanced bandpass filter with continuously high common-mode suppression," *ACES Jour.*, vol. 28, no. 7, pp. 628-632, July 2013.
- [10] Q. Xiao and C. X. Zhou, "Design of balanced SIW filter with transmission zeroes and linear phase," *ACES Jour.*, vol. 30, no. 9, pp. 1019-1023, Sep. 2015.
- [11] W. R. Eisenstant, B. Stengel, and B. M. Thompson, *Microwave Differential Circuit Design Using Mixed-Mode S-Parameters*. Boston, MA: Artech House, 2006.
- [12] Y. X. Guo, Z. Y. Zhang, and L. C. Ong, "Improved wide-band Schiffman phase shifter," *IEEE Trans. Microw. Theory Techn.*, vol. 54, no. 3, pp. 2412-2418, Mar. 2006.



a postgraduate.

Chaoying Zhao was born in Wuhu, Anhui Province, China, in 1992. She received the B.E. degree from the Shandong University, Weihai, China, in 2014. From October 2014, she went to Nanjing University of Science and Technology (NUST), Nanjing, China, for further study as

Her research interests include ultra-wideband (UWB) circuits and technologies, power dividers and planar microstrip filters.



Wenjie Feng was born in Shangqiu, Henan Province, China, in 1985. He received the B.Sc. degree from the First Aeronautic College of the Airforce, Xinyang, China, in 2008, the M.Sc. and Ph.D. degrees from the Nanjing University of Science and Technology (NUST), Nanjing, China, in 2010, 2013.

From November 2009 to February 2010, March 2013 to September 2013, he was a Research Assistant with the City University of Hong Kong. From October 2010 to March 2011, he was an exchange student with the Institute of High-Frequency Engineering, Technische Universität München, Munich, Germany. He is currently an Associate Professor with the Nanjing University of Science and Technology, Nanjing, China. He has authored or co-authored over 100 internationally referred journal and conference papers. His research interests include ultra-wideband (UWB) circuits and technologies, substrate integrated components and systems, planar microstrip filters and power dividers, LTCC circuits.

Feng is a Reviewer for over ten internationally referred journal and conference papers, including eight IEEE Transactions and Letters. He serves as an Associate Editor for the International Journal of Electronics from 2015.



Yuan Chun Li was born in Anhui Province, China. She received the B.S. degree in Electronic Engineering from Anhui University, Hefei, China, in 2006, the M.S. degree in Electronic Engineering from University of Science and Technology of China, Hefei, China, in 2009, and the Ph.D.

degree in Electronic Engineering from the City University of Hong Kong, Kowloon, Hong Kong.

From Oct 2012 to Jun 2015, she was a Research Fellow with the City University of Hong Kong. She is currently an Associate Professor with the School of Electronic and Information Engineering, South China University of Technology. Her research interests include RF and microwave passive and active circuits, and monolithic microwave integrated circuits.



Wenquan Che received the B.Sc. degree from the East China Institute of Science and Technology, Nanjing, China, in 1990, the M.Sc. degree from the Nanjing University of Science and Technology (NUST), Nanjing, China, in 1995, and the Ph.D. degree from the City University of Hong Kong (CITYU), Kowloon, Hong Kong, in 2003.

In 1999, she was a Research Assistant with the City University of Hong Kong. From March 2002 to September 2002, she was a Visiting Scholar with the Polytechnique de Montréal, Montréal, QC, Canada. She is currently a Professor with the Nanjing University of Science and Technology, Nanjing, China. From 2007 to 2008, she conducted academic research with the Institute of High Frequency Technology, Technische Universität München. During the summers of 2005–2006 and 2009–2012, she was with the City University of Hong Kong, as Research Fellow and Visiting Professor. She has authored or co-authored over 110 internationally referred journal papers and over 60 international conference papers. She has been a Reviewer for *IET Microwaves, Antennas and Propagation*. Her research interests include electromagnetic computation, planar/coplanar circuits and subsystems in RF/microwave frequency, microwave monolithic integrated circuits (MMICs) and medical application of microwave technology.

Che is a Reviewer for the IEEE Transactions on Microwave Theory and Techniques, IEEE Transactions on Antennas and Propagation, IEEE Transactions on Industrial Electronics, and IEEE Microwave and Wireless Components Letters. She was the recipient of the 2007 Humboldt Research Fellowship presented by the Alexander von Humboldt Foundation of Germany, the 5th China Young Female Scientists Award in 2008 and the recipient of Distinguished Young Scientist awarded by the National Natural Science Foundation Committee (NSFC) of China in 2012.